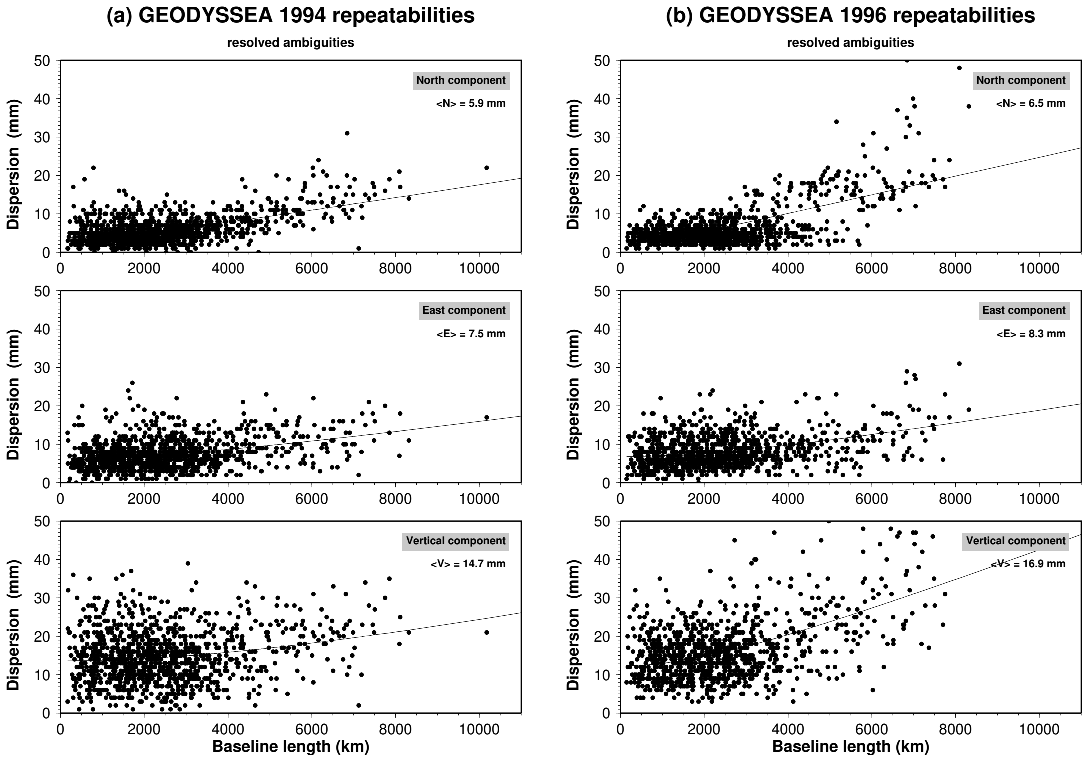

Figure 1: Repeatabilities of the GEODYSSEA 1994 $^{(a)}$ and 1996 $^{(b)}$ GPS campaigns. Every baseline in the network is measured 5 times (one time is one day solution). The mean baseline value is computed from those 5 "measures" and then the dispersion of those measures about their mean. The repeatability plot show the value of this dispersion (RMS) plotted against baseline length. The line running through the "cloud" of points indicates the mean value of the dispersion as a function of baseline length. The values in brackets (upper right corner of each box) give the mean value of the repeatability averaged over all baselines. 96 overall repeatabilities do not differ significantly from 94 repeatabilities. Horizontal values are in between 6 and 8 mm, where vertical values reach 15 mm. Nevertheless, the degradation of the repeatabilities as baseline length increases is more pronouced in the 96 data than in the 94. In principle, this is due to better orbits in 94 than in 96.

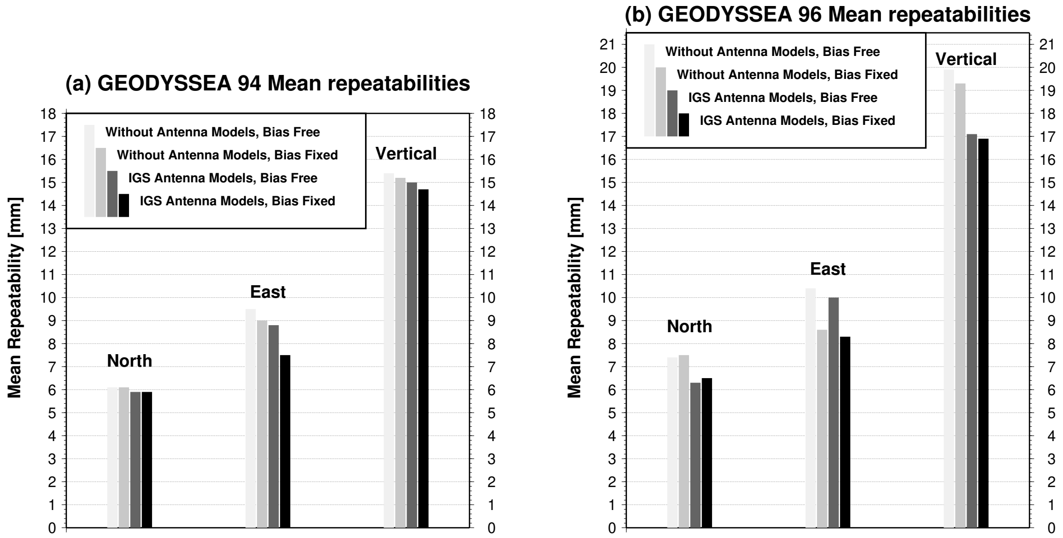

Figure 2: Mean repeatabilities of the GEODYSSEA 1994 $^{(a)}$ and 1996 $^{(b)}$ GPS campaigns. For each figure, the first, second and third bunch of 4 bars stand for the North, East and Vertical components. For every component, the 4 bars show the mean repeatability obtained with 4 different solutions: with and without antenna phase center models, and with and without ambiguity resolution. It is clear that applying both, eg. using antenna models and solving for integer ambiguities, improve the overall repeatability of the 94 solution. For the 96 data set, the "bias fixing" scheme is particularly successfull in improving the East component repeatability (in average 2 mm lower) and the antenna phase center models improve the vertical component by again about 2mm (which is still 2mm higher than in 94).

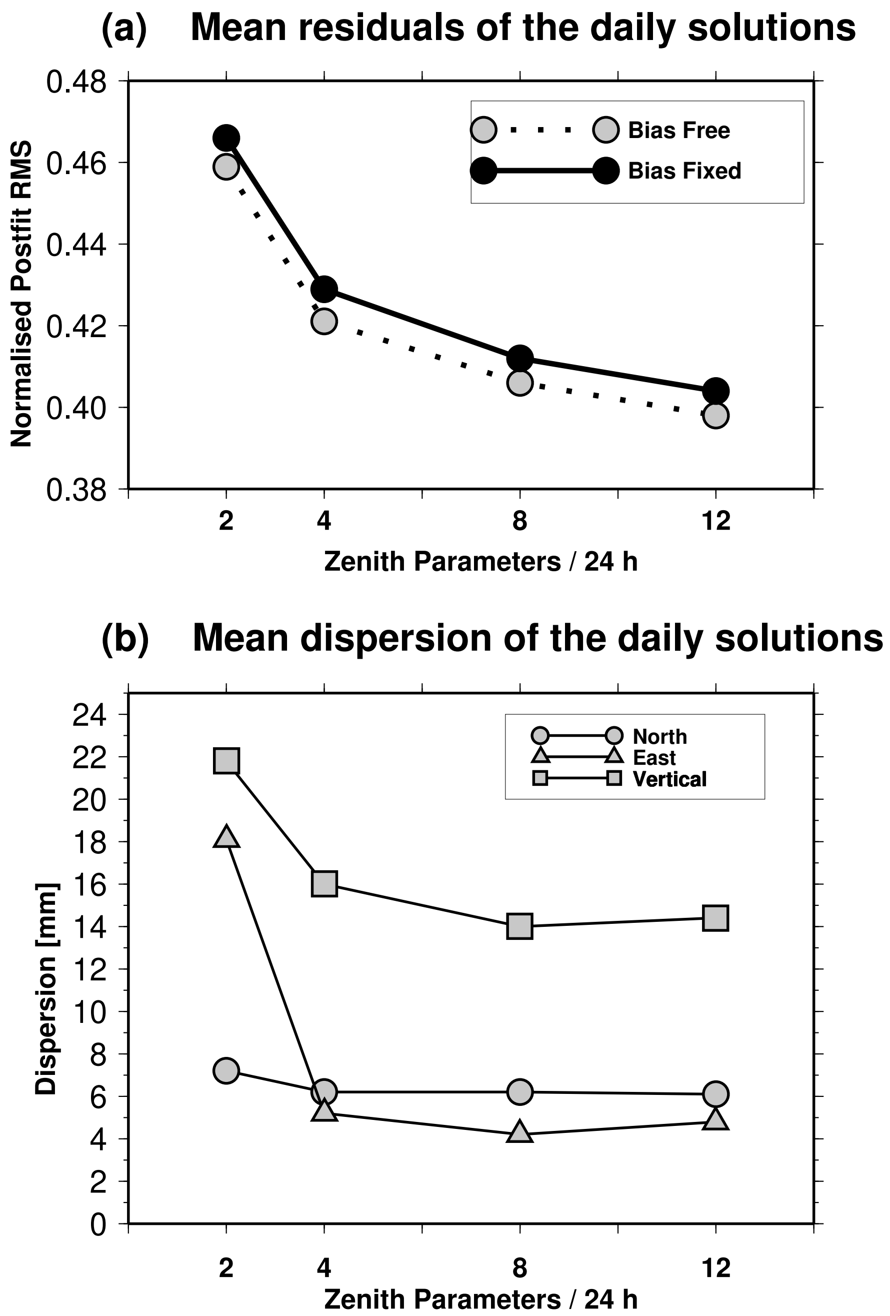

Figure 3: Residuals [a] and dispersion [b] of the 1994 daily solutions as a function of the number of daily zenith parameters. GPS measurements are affected by the wave propagation through the atmosphere lower layer (the troposphere). To take into account the fact that propagation conditions in the troposphere actually change with time, a new "zenith parameter" is estimated every period of time (ie. 3 hours). 1 to 12 parameters are estimated every day (from 1 for 24 hours to 1 every 2 hours). fig a) shows that, as expected, postfit rms of the daily solutions decrease when more parameters are estimated. Fig b) shows that a dramatic inprovement of the East component repeatability is obtained when at least 4 parameters are estimated every 24 hours (1 every 6 hours). A good compromise for good repeatabilities, "robust" solutions, and reasonnable computing time is obtained for 8 parameters per day (1 every 3 hours).

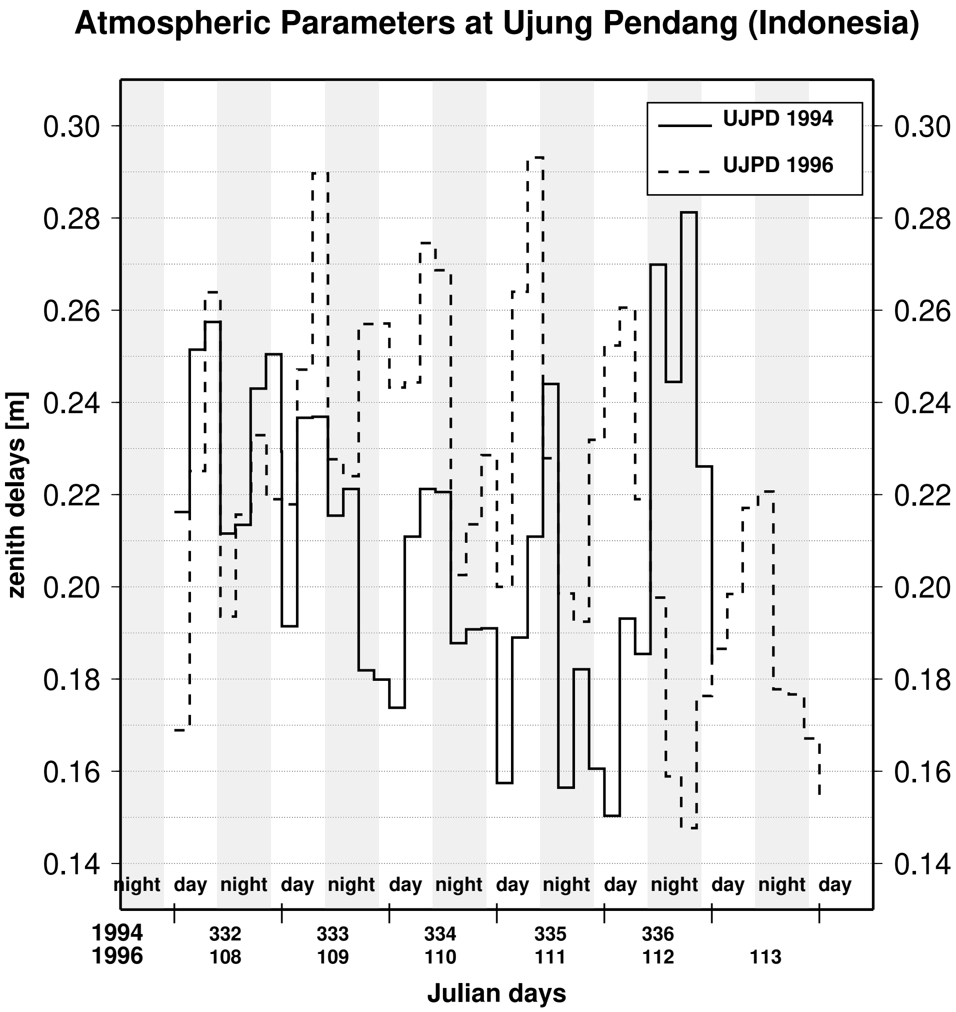

Figure 4: Zenith delay parameters estimated at station UJPD (Ujung Pendang, Indonesia) as a function of time. Maximum variations from one parameter to the following (ie. every 3 hours) reach 9 cm in both 1994 and 1996 data. The 1994 data show a steady decrease of the daily average (from 23 cm to 17 cm) during most of the observation time span (4.5 days). On the opposite, the 1996 data show higher long term variations: from 20 cm to 26 cm the first 3 days, and then from 26 cm to 18 cm the last 3 days). Noiser troposphere at many sites could be the clue to the slightly degraded vertical repeatabilities in the 1996 (April) data analysis compared to 1994 (November).

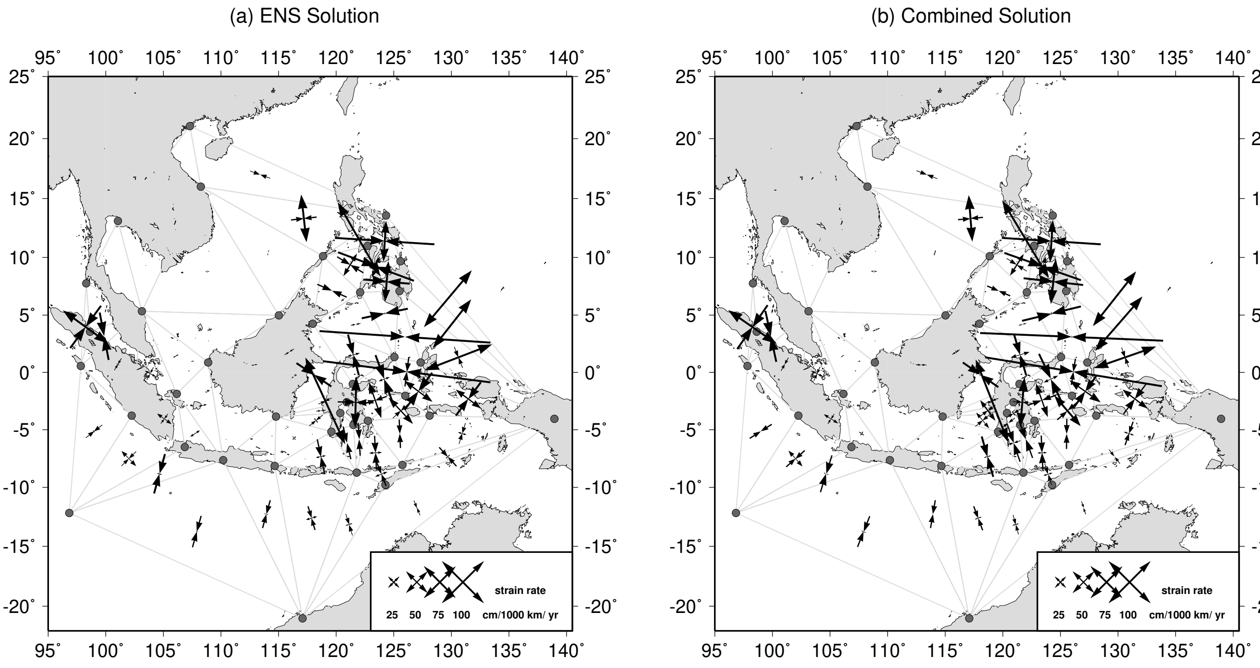

Figure 5: Strain rates computed from the ENS [(a)] GEODYSSEA solution and the combined [(b)] solution. Inward arrows indicate compression, outward arrows indicate extension. Strains with uncertainties higher than their amplitude are not represented. The differences between the two solutions are marginals. In fact, the differences are smaller than 5mm / 1000km / year (approximately 5 ppb per year).

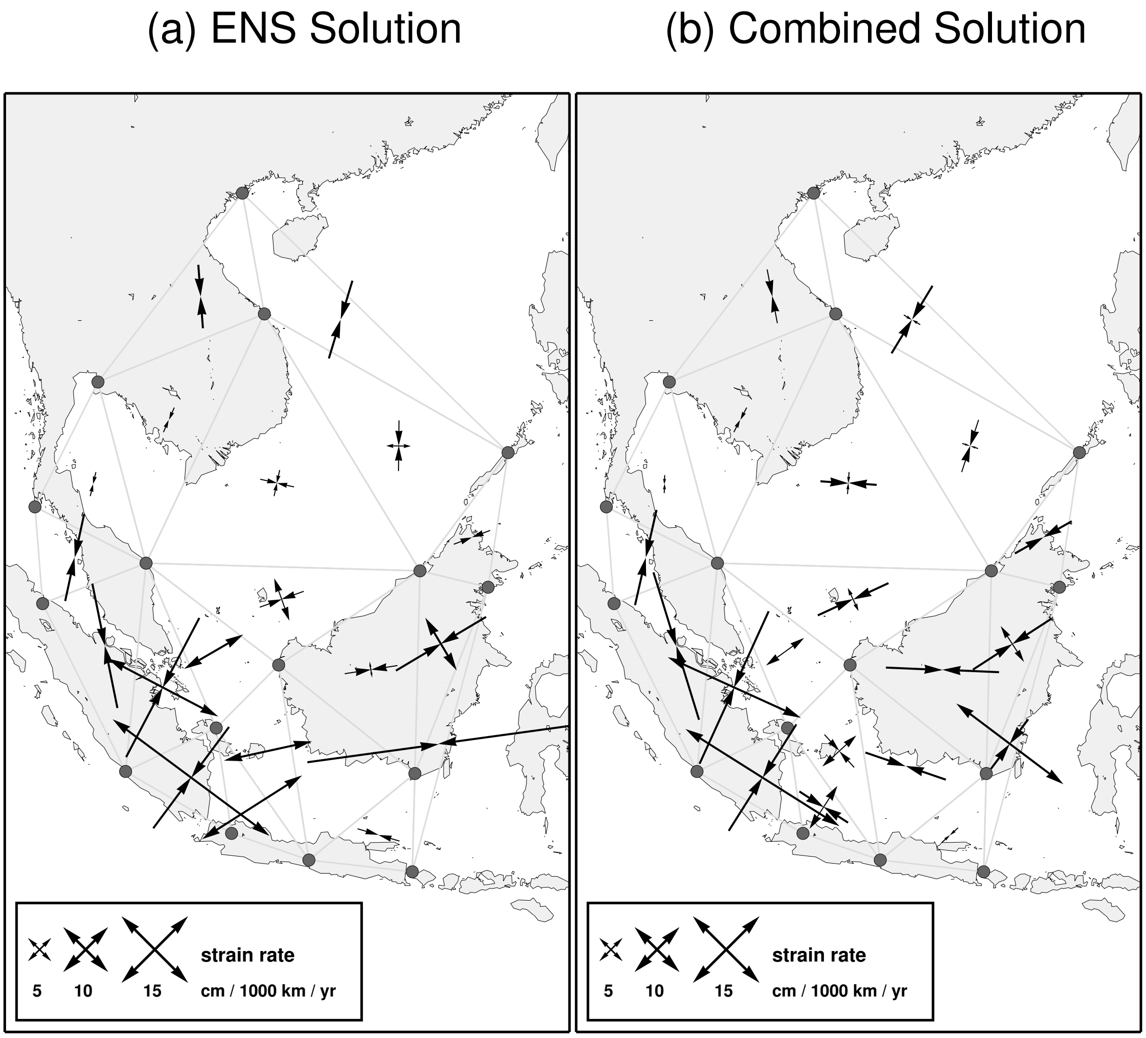

Figure 6: Strain rates in the South China Sea. Comparison between the ENS [(a)] and the combined [(b)] solution. In this area where deformation are very small (one order of magnitude less than in the rest of the network : < 10mm / 1000km / yr), the two solutions show some slight differences. The largest discrepancy lie in the BATU-BALI-TAWA triangle where the ENS solution shows E-W compression and the combined solution shows NW-SE extension. The stretched shape of this triangle makes it particularly sensitive to errors, opposite to a true Delauney (equilateral) triangle. From the comparison, we can estimate the uncertainty of deformation rates (internal to the GEODYSSEA network) to be around 5 ppb per year or 5 mm/yr on a 1000 km baseline.

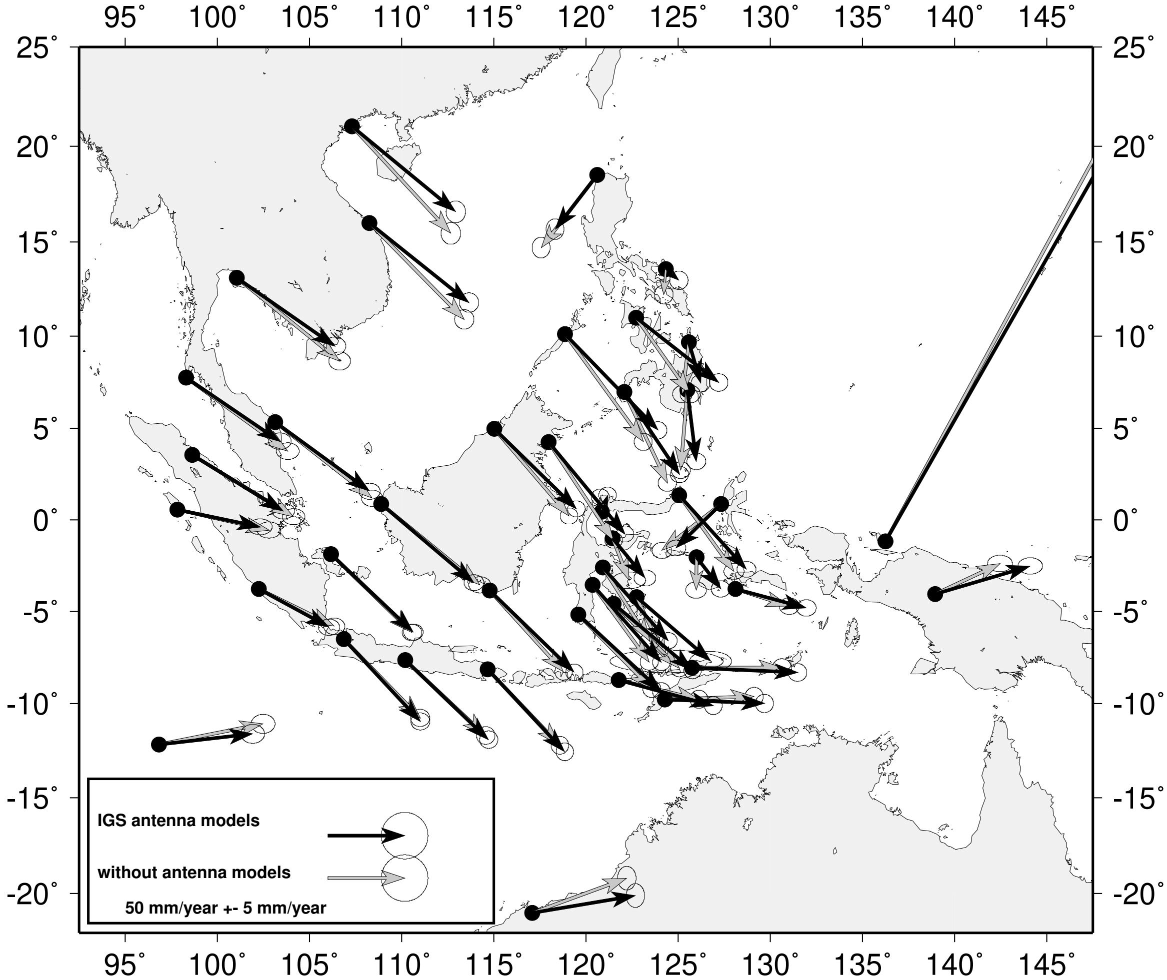

Figure 7: Comparison of velocities obtained in a totally free network adjustment, with and without antenna phase center models. In both cases constraints on stations are 1 meter on positions and 20/50 centimeter per year on the horizontal/vertical velocities. Formal uncertainties are shown by 99% confidence ellipses. Velocities computed with antenna phase center models are similar to the "crude" velocities, but differences can be as high as 1 cm/yr for some sites. Nevertheless, velocities computed with different antenna models (Schupler tables, not shown here), lie in between the 2 solutions, closer to the one obtained with IGS tables. The later confirms that applying antenna models leads to more accurate results, although those models are not definitive.

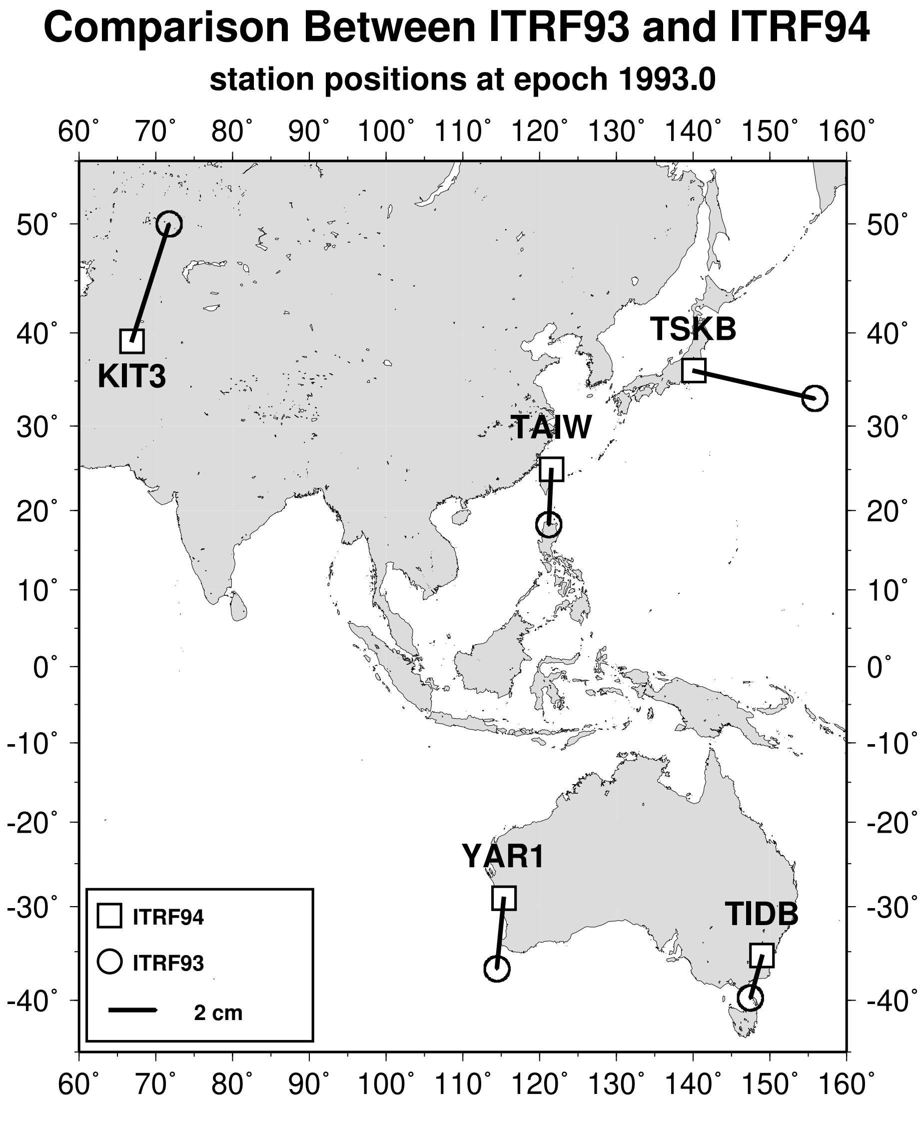

Figure 8: Comparison of station positions at epoch 1994.9 (the GEODYSSEA 1^{st} campaign) between ITRF93 and ITRF94. Open squares are for station positions in ITRF94, open circles for ITRF93. The grey squares show station positions estimated in the ITRF93 **solution**, rotated in the ITRF94 **reference frame**. Part of the difference in the station positions is accounted by the known transformation parameters from one reference frame to the other (Taiw, Yar1, Tidb), but other station positions (Kit3, Tskb) are clearly estimated differently in the 2 solutions.

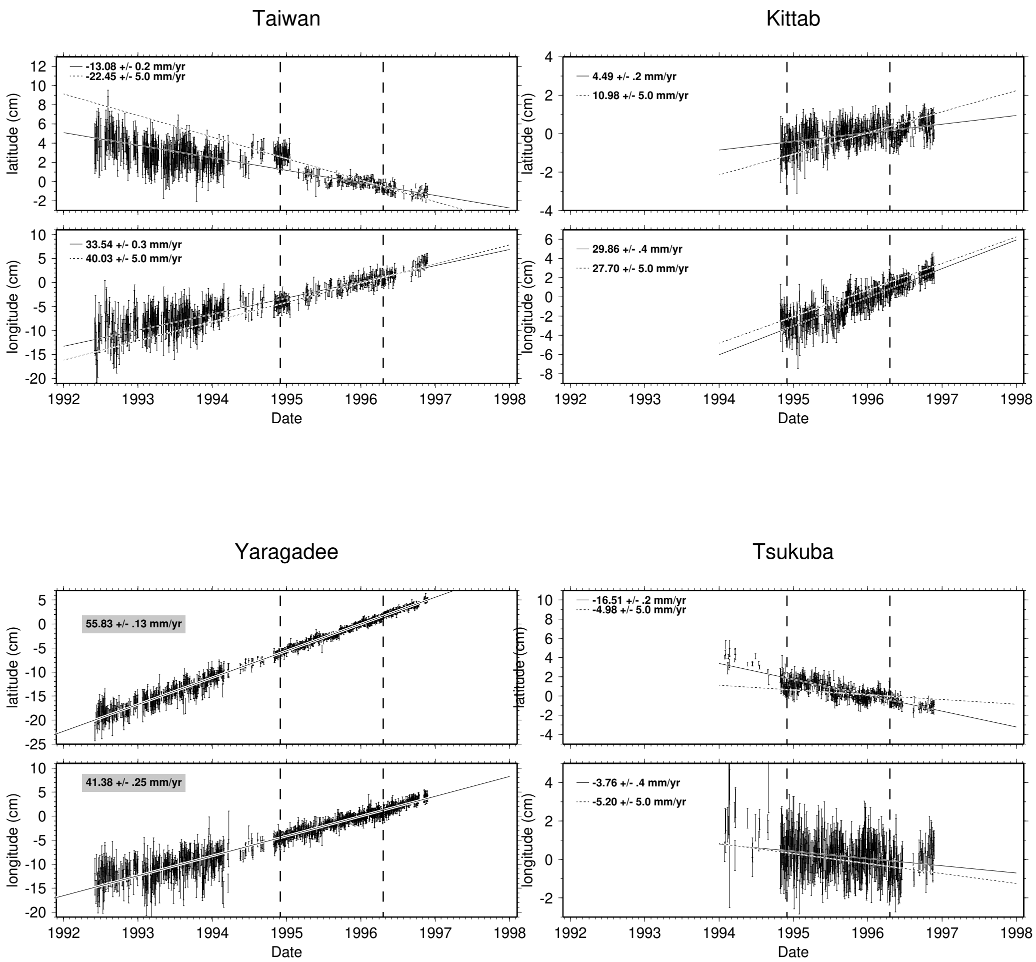

Figure 9: Time series from JPL daily GPS solutions for 4 out of the 5 IGS stations included in the GEODYSSEA solution. The daily position of every stations (in ITRF94) are simply plotted against time. For each station, the upper box show the latitudinal (North) component, and the lower box show the longitudinal (East) component. The epochs of the GEODYSSEA campaigns are indicated by the vertical dashed lines at December 94 and April 96. The solid lines indicate the rates inferred from the total time series when the dashed lines indicate the rates inferred taking only a bunch of days around the GEODYSSEA campaign dates, i.e. simulating epoch-like campaigns. If the agreement is quite good for the Australian stations Yarragadee and Canberra (not shown here), the other clearly show a high discrepancy (as high as 50% or 10 mm/yr).

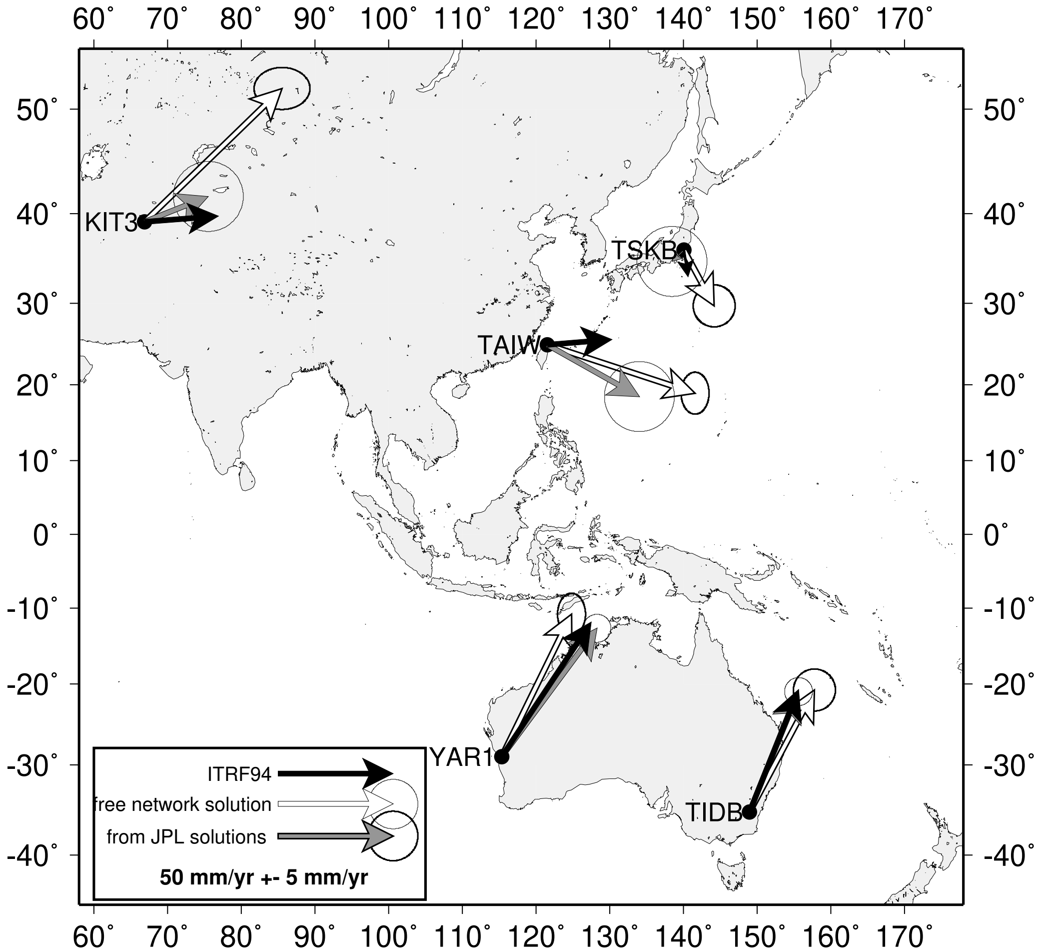

Figure 10: Comparison of the velocities from the ENS free network solution, velocities simulated from JPL times series, and the ITRF94 velocities for the 5 IGS stations included in the GEODYSSEA network. In order to facilitate the comparison, the free network solution is rotated in the ITRF94, using the 2 australian velocities which match quite well. There are obvious discrepancies between long-term velocities ("ITRF94"), and instantaneous velocities ("JPL") inferred from epoch-like campaigns, at stations Kittab, Taiwan, and Tsukuba. At the last two stations, the GEODYSSEA solution is in better agreement with the "JPL" velocities than with the "ITRF94". Kittab is a problem only in the ENS solution, which is therefore eliminated by the combination approach of the official GEODYSSEA solution.